Noname manuscript No.
(will be inserted by the editor)

Characteristics of rogue waves on a soliton background of the vector Lakshmanan-Porsezian-Daniel equation

Min-Jie Dong · Li-Xin Tian

Received: date / Accepted: date

Abstract In this paper, the semi-rational solutions that causes vector rogue waves and breathers can be obtained by using the Darboux dressing transformation. We studied vector rogue waves and the interaction between rogue waves and light-dark solitons, and observed that during the interaction, due to the interference between the light-dark components of the solitons, a respiration-like structures appears. Besides, it can be observed that the rogue waves and soliton merge together. Moreover, the main characteristics of the interactions between the breathers and bright-dark solitons are displayed with some graphics.

Keywords Solitons, Rogue waves, The vector Lakshmanan-Porsezian-Daniel equation.

PACS 35Q51, 35Q53, 35C99, 68W30, 74J35

(Some figures in this article are in colour only in the electronic version)

1 Introduction

Rogue waves refer to transient huge waves with extremely large amplitude that seem to be everywhere and responsible for a large number of shipwrecks[1,2]. Recently, more and more scholars are devoted to studying such rare extreme events in the fields

This work was supported by the National Natural Science Foundation of China No. 71690242, No. 11731014.

Min-Jie Dong (⊠)
School of Mathematical Sciences, Nanjing Normal University, Nanjing, Jiangsu, China
E-mail: dongminjiepoppy@126.com

Li-Xin Tian
School of Mathematical Sciences, Nanjing Normal University, Nanjing, Jiangsu, China
Nonlinear Scientific Research Center, Jiangsu University, Zhenjiang, Jiangsu, China
E-mail: tianlx@ujs.edu.cn

of hydrodynamics[3], capillary waves[4], plasma physics[5], Bose-Einstein condensates[6] and even financial system [7,8]. Due to its wide application, the nonlinear Schrödinger(NLS) equation has attracted widespread attentions [9–15]. The topic of research is the common characteristics and differences manifestations of rogue waves in different backgrounds. According to research, the appearance of rogue waves depends on the instability of modulation[16]. Characteristics of rogue waves and lumps in certain optical fibers or fluids can be described by rational solutions of NLS equation, which has certain types of breathers or solitons in finite backgrounds. The breather solutions contain two special cases: (1) Akhmediev breathers (AB)[17], which is localized in the propagation direction and possess the periodicity in the temporal direction; (2) Kuznetsov-Ma (KM) [18]solitons, which is localized in the temporal dimension but periodicity in the propagation direction.

In this paper, we give the Darboux-dressing transformation to construct the breather solutions and semirational solutions of the vector Lakshmanan-Porsezian-Daniel (LPD) equation[19,20].

$$\begin{cases} iq_{1t} + \dfrac{1}{2}q_{1xx} + q_1A + \sigma[q_{1xxxx} + 4q_{1xx}A + 2q_{1x}(A_x + 2B) + 2q_1(3A^2 + B_x^* + 2C)] = 0, \\ iq_{2t} + \dfrac{1}{2}q_{2xx} + q_2A + \sigma[q_{2xxxx} + 4q_{2xx}A + 2q_{2x}(A_x + 2B) + 2q_2(3A^2 + B_x^* + 2C)] = 0, \end{cases} \tag{1}$$

where $A = |q_1|^2 + |q_2|^2$, $B = q_{1x}q_1^* + q_{2x}q_2^*$, and $C = q_{1xx}q_1^* + q_{2xx}q_2^*$. In the optical environment, q_1 and q_2 are the complex envelopes of two field polarization components, where t is the propagation distance , x is the delay time. The superscripts denote the complex conjugate and the subscripts represent the partial derivatives.

The parameter $\sigma = 0$ scales the perturbation to a coupled NLS equation or Manakov system[21,22],which only consider the group velocity dispersion and Kerr nonlinearity

$$\begin{cases} iq_{1t} + \dfrac{1}{2}q_{1xx} + q_1(|q_1|^2 + |q_2|^2) = 0, \\ iq_{2t} + \dfrac{1}{2}q_{2xx} + q_2(|q_1|^2 + |q_2|^2) = 0, \end{cases} \tag{2}$$

where $q_1(x,t)$ and $q_2(x,t)$ are complex valued functions. In the past decades, much work have been done for (2) : Chen and Mihalache used a nonrecursive Darboux transformation formalism to obtain the hierarchy of the rogue wave solution [21]; Wang and Han studied on rogue waves on a soliton background by the DDT method [22].

Compared with the Manakov system, the vector LPD model have higher accuracy and considers the additional items of self-steepening effect, fourth-order dispersion effect, fifth-order nonlinearity and higher-order nonlinear dispersion, so it can describe the propagation of a few periodic ultrashort pulses in the optical fiber[19]. In this paper, choosing $\sigma = 1$, our general solution reproduces known rogue waves of equation (1) via the Darboux dressing transformation (DDT) at special parameter values, such as vectors Peregrine soliton and bright- and dark-rogue waves. In Section 2, recall the essential steps of the DDT of the equation (1). In Section 3, based on the obtained DDT, the complicated first-order breather wave and rogue wave solutions for equation (1) are systematically derived. In Section 4, the higher-order rogue

waves are considered. Our conclusions will be given in Section 5. Additionally, the main features of these solutions are graphically analyzed.

2 Lax pair and the DDT

Due to the equation (1) is completely integrable[20], its Lax Pair yields[19]

$$\begin{cases} \Phi_x = M\Phi = (-i\lambda\varrho_3 + R), \\ \Phi_t = N\Phi = (8\lambda^3 M + 2i\lambda^2(E + 2T\varrho_3) + 2\lambda(2R^3 + 2R_xR + T_x) \\ \qquad - \lambda R - i[(T_{xx} + 3T^2) + \dfrac{T}{2}]\varrho_3)\Phi. \end{cases} \tag{3}$$

where $\Phi = (\phi_1, \phi_2, \phi_3)'$ ($'$ mens a matrix transpose) is the vector eigenfunction of the parameter λ, ϕ_1, ϕ_2 and ϕ_3 are the complex functions of (x, t), and $i^2 = -1$, $E = diag(1, 0, 0)$,

$$\varrho_3 \begin{pmatrix} 1 & 0 & 0 \\ 0 & -1 & 0 \\ 0 & 0 & -1 \end{pmatrix}, \qquad R = \begin{pmatrix} 0 & u_1^* & u_2^* \\ -u_1 & 0 & 0 \\ -u_2 & 0 & 0 \end{pmatrix}, \qquad T = \begin{pmatrix} |q_1|^2 + |q_2|^2 & -q_{1x}^* & -q_{2x}^* \\ q_{1x} & |q_1|^2 & q_1 q_2^* \\ q_{2x} & q_1^* q_2 & |q_2|^2 \end{pmatrix}. \tag{4}$$

where the superscript $*$ representing the complex conjugate, λ being the spectral parameter. From the compatibility condition $M_t - N_x + MN - NM = 0$, equation (1) can be easily obtained.

Based on the study of [23–27], the DDT for equation (1) can be derived.

Theorem 1 *The following unified DT yields*

$$\Phi_{[1]} = K\Phi, \qquad K = I_3 - \frac{\lambda_1 - \lambda_1^*}{\lambda - \lambda_1^*} P_1, \tag{5}$$

where

$$P_1 = \frac{\Lambda_0 \Lambda_0^\star}{\Lambda_0^\star \Lambda_0}, \qquad \Lambda_0 = \Phi(x, t, \lambda_1) Z_0 = \begin{pmatrix} h_0 \\ h_1 \\ h_2 \end{pmatrix}, \tag{6}$$

and $I_3 = diag(1, 1, 1)$, Φ is a special vector for the lax pair with $\lambda = \lambda_1$, and $\star$ represent Hermitian conjugation. Obviously, the linear system (3) *can be rewritten in another form*

$$\Phi_{[1]x} = M_{[1]}\Phi_{[1]}, \qquad \Phi_{[1]t} = N_{[1]}\Phi_{[1]}. \tag{7}$$

and transformation between potential functions reads

$$q_{[1]} = q_{[0]} + i(\lambda_1^* - \lambda_1)[P_1, \varrho_3] \tag{8}$$

or

$$\begin{pmatrix} q_{1,[1]} \\ q_{2,[1]} \end{pmatrix} = \begin{pmatrix} q_{1,[0]} \\ q_{2,[0]} \end{pmatrix} + \frac{2i(\lambda_1^* - \lambda_1)h_0^*}{|h_0|^2 + |h_1|^2 + |h_2|^2} \begin{pmatrix} h_1 \\ h_2 \end{pmatrix} \tag{9}$$

Where commutator $[P_1, \varrho_3] = P_1\varrho_3 - \varrho_3 P_1$.

3 Breather wave solutions

To derive the rogue wave solutions for equation (1), we start from the seed solution-nonzero plane wave solution. We denote them as

$$q_j = c_j \exp(a_1 x + b_1 t), \qquad j = 1, 2, \tag{10}$$

where c_j,a_1 and b_1 are constants. After the simple calculation, we can obtain a constraint relationship

$$b_1 = a_1^4 - 12a_1^2(c_1^2 + c_2^2) + 6(c_1^2 + c_2^2)^2 - \frac{1}{2}a_1^2 + c_1^2 + c_2^2. \tag{11}$$

where a_1 is the real amplitudes and b_1 is the wave numbers, which are taken to be real. Based on the Ref.[25], the corresponding solution of the Lax pair can be sought in a new form

$$\Phi = \begin{pmatrix} h_0(x,t) \\ h_1(x,t) \\ h_2(x,t) \end{pmatrix} = \Delta PQZ, \qquad P = \exp(i\breve{M}x), \qquad Q = \exp(i\breve{N}x), \tag{12}$$

$$\Delta = diag(1, \exp(i\varphi), \exp(i\varphi)), \qquad Z = (\alpha_1, \alpha_2, \alpha_3)^{'},$$

where α_1, α_2 and α_3 are arbitrary complex. Substituting equation (35) into the Lax pair, $\breve{M}$ and $\breve{N}$ obatined

$$\breve{M} = \begin{pmatrix} -\lambda & -ic_1 & -ic_2 \\ ic_1 & \lambda - a_1 & 0 \\ ic_2 & 0 & \lambda - a_1 \end{pmatrix}, \tag{13}$$

$$\breve{N} = N_0 + N_1\lambda + N_2\lambda^2 + N_3\lambda^3 + N_4\lambda^4, \tag{14}$$

where

$$N_4 = -8\lambda^4\varrho_3,$$

$$N_3 = 8i\lambda^3 \begin{pmatrix} 0 & -c_1 & -c_2 \\ c_1 & 0 & 0 \\ c_2 & 0 & 0 \end{pmatrix}, \qquad N_2 = \begin{pmatrix} 4c_1^2 + 4c_2^2 + 2 & -4ic_1a_1 & -4ic_2a_1 \\ 4ic_1a_1 & -4c_1^2 & -4c_1c_2\sigma \\ 4ic_2a_1 & -4c_1c_2 & -4c_2^2 \end{pmatrix},$$

$$N_1 = \begin{pmatrix} N_{1[11]} & N_{1[12]} & N_{1[13]} \\ -N_{1[12]} & N_{1[22]} & N_{1[23]} \\ -N_{1[13]} & N_{1[23]} & N_{1[33]} \end{pmatrix}, \qquad N_0 = \begin{pmatrix} N_{0[11]} & N_{0[12]} & N_{0[13]} \\ -N_{0[12]} & N_{0[22]} & N_{0[23]} \\ -N_{0[13]} & N_{0[23]} & N_{0[33]} \end{pmatrix},$$

$$N_{1[11]} = 4\omega a_1, \qquad N_{1[12]} = -\frac{ic_1}{2}(4a_1^2 - 8\omega - 2), \qquad N_{1[13]} = -\frac{ic_2}{2}(4a_1^2 - 8\omega - 2),$$

$$N_{1[22]} = -4c_1^2a_1, \qquad N_{1[23]} = -4c_1c_2a_1, \qquad N_{1[33]} = -4c_2^2a_1,$$

$$N_{0[11]} = -3\omega^2 + 3a_1^2\omega - \frac{1}{2}\omega, \qquad N_{0[12]} = -\frac{ic_1}{2}(2a_1^3 - 12a_1\omega - a_1),$$

$$N_{0[13]} = -\frac{ic_2}{2}(2a_1^3 - 12a_1\omega - a_1), \qquad N_{0[23]} = \frac{c_1c_2}{2}(6a_1^2 - 6\omega - 1),$$

$$N_{0[22]} = -3c_1^4 - 9c_1^2c_2^2 + 9a_1^2c_1^2 - a_1^4 + 12a_1^2c_2^2 - 6c_2^4 - \frac{c_1^2}{2} + \frac{a_1^2}{2} - c_2^2,$$

$$N_{0[33]} = -3c_2^4 - 9c_1^2c_2^2 + 9a_1^2c_2^2 - a_1^4 + 12a_1^2c_1^2 - 6c_1^4 - \frac{c_2^2}{2} + \frac{a_1^2}{2} - c_1^2,$$

and $\omega^2 = c_1^2 + c_2^2$. By using maple software, we can obtain the detailed result of P and Q.

After complicated calculations, the matrices P can be written as

$$P = \exp(-\frac{ia_1x}{2})\begin{pmatrix} P_{[11]} & 2c_1\tau^{-1}\sinh(\frac{x\tau}{2}) & 2c_2\tau^{-1}\sinh(\frac{x\tau}{2}) \\ -2c_1\tau^{-1}\sinh(\frac{x\tau}{2}) & P_{[22]} & P_{[23]} \\ -2c_2\tau^{-1}\sinh(\frac{x\tau}{2}) & P_{[23]} & P_{[33]} \end{pmatrix}, \tag{15}$$

where

$$\begin{cases} P_{[11]} = -\dfrac{(2i\lambda - ia_1)\sinh(\frac{x\tau}{2}) - 2\tau\cosh(\frac{x\tau}{2})}{\tau}, \\ P_{[22]} = -\dfrac{c_1^2}{\tau\omega}((-2i\lambda + ia_1)\sinh(\frac{x\tau}{2}) - \tau\cosh(\frac{x\tau}{2})) + \dfrac{c_2^2}{\omega}\exp(i\lambda x - \dfrac{ixa_1}{2}), \\ P_{[33]} = -\dfrac{c_2^2}{\tau\omega}((-2i\lambda + ia_1)\sinh(\frac{x\tau}{2}) - \tau\cosh(\frac{x\tau}{2})) + \dfrac{c_1^2}{\omega}\exp(i\lambda x - \dfrac{ixa_1}{2}), \\ P_{[23]} = -\dfrac{c_1c_2}{\tau\omega}((-2i\lambda + ia_1)\sinh(\frac{x\tau}{2}) - \tau\cosh(\frac{x\tau}{2})) - \dfrac{c_1c_2}{\omega}\exp(i\lambda x - \dfrac{ixa_1}{2}), \\ \omega^2 = c_1^2 + c_1^2, \qquad \tau = \sqrt{-4\lambda^2 + 4\lambda a_1 - a_1^2 - 4\omega}. \end{cases} \tag{16}$$

Similarly, the exponential matrices Q can be written as

$$Q = \begin{pmatrix} Q_{[11]} & Q_{[12]} & Q_{[13]}) \\ -Q_{[12]} & Q_{[22]} & Q_{[23]}) \\ -Q_{[13]} & Q_{[23]} & Q_{[33]}) \end{pmatrix}, \tag{17}$$

where

$$\begin{cases} Q_{[11]} = \dfrac{-1}{\upsilon}(\varpi\sinh(\frac{t\upsilon}{4}) + \upsilon\cosh(\frac{t\upsilon}{4}))\exp(i\frac{t\eta}{4}), \\ Q_{[1j]} = \dfrac{2c_{j-1}}{\upsilon}((16\lambda^3 + 8\lambda^2a_1 + 4\lambda a_1^2 - 8\lambda\omega + 2a_1^3 - 12a_1\omega - 2\lambda - a_1)\sinh(\frac{t\upsilon}{4})\exp(i\frac{t\eta}{4}), \\ Q_{[22]} = \dfrac{c_1^2}{\upsilon\omega}(\varpi\sinh(\frac{t\upsilon}{4}) + \upsilon\cosh(\frac{t\upsilon}{4}))\exp(i\frac{t\eta}{4}) + \dfrac{c_2^2\exp(i\theta t)}{\omega}, \\ Q_{[23]} = \dfrac{c_1c_2}{\upsilon\omega}(\varpi\sinh(\frac{t\upsilon}{4}) + \upsilon\cosh(\frac{t\upsilon}{4})\exp(i\frac{t\eta}{4})) - \dfrac{c_1c_2\exp(i\theta t)}{\omega}, \\ Q_{[33]} = \dfrac{c_2^2}{\upsilon\omega}(\varpi\sinh(\frac{t\upsilon}{4}) + \upsilon\cosh(\frac{t\upsilon}{4}))\exp(i\frac{t\eta}{4}) + \dfrac{c_1^2\exp(i\theta t)}{\omega}, \\ \varpi = 32i\lambda^4 - 16i\lambda^2\omega - 16i\lambda a_1\omega - 2ia_1^4 + 12ia_1^2\omega - 4i\lambda^2 + ia_1^2, \\ \upsilon = \tau(16\lambda^3 + 8\lambda^2a_1 + 4\lambda a_1^2 - 8\lambda\omega + 2a_1^3 - 12a_1\omega - 2\lambda - a_1), \\ \eta = -2a_1^4 + 24a_1^2\omega - 12\omega^2 + 4\lambda^2 + a_1^2 - 2\omega, \\ \theta = 8\lambda^4 - a_1^4 + 12a_1^2\omega - 6\omega^2 + \dfrac{1}{2}a_1^2 - \omega. \end{cases} \tag{18}$$

According the equation (35), the seed solution (10) and **Theorem 1**, the new rational solution composed of exponential and hyperbolic functions is easily obtained.

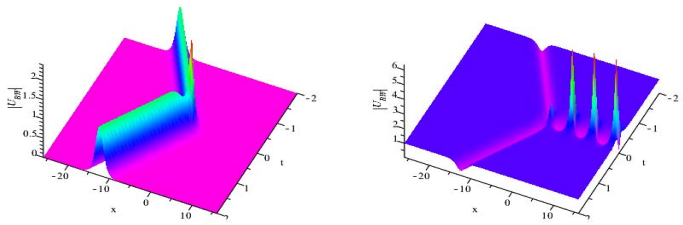

(**a**) (**b**)

Fig. 1 (Color online) AB in the vector Lakshmanan-Porsezian-Daniel equation (1)for parameters: $c_1 = 0, c_2 := 1, \lambda := \frac{1}{2}i, h_0 = h_1 = h_2 = 1$.

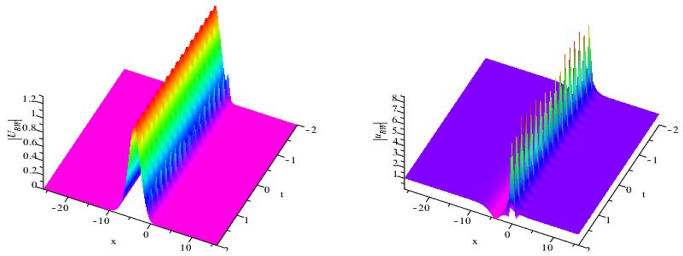

(**a**) (**b**)

Fig. 2 (Color online) KM in the vector Lakshmanan-Porsezian-Daniel equation(1) for parameters: $c_1 = 0, c_2 := 1, \lambda := \frac{6}{5}i, h_0 = h_1 = h_2 = 1$.

Since the expression is too long, it is omitted here. The dynamic characteristics of the equation (1) still shown in Figure 1 and Figure 2.

As seen in Fig.1 and Fig.2, they are dynamic characteristics depicted by choosing the suitable parameters. Fig. 1(a) and (b) display the bright soliton and dark solutions coexist with the AB soliton, respectively. Fig. 2 displays the KM propagation on a plane wave background and bright-dark soliton background.

Taking $\lambda = \frac{1}{2}a_1 \pm i\omega$, the function $\exp(i\check{M}x + i\check{N}t)$ can be transformed combination of exponential and polynomial functions of (x, t). In this work, choosing $\lambda = \frac{1}{2}a_1 + i\omega$, and using Taylor expansion

$$sin(x) = x - \frac{x^3}{3} + \frac{x^5}{5!} + \cdots, \qquad cos(x) = 1 - \frac{x^2}{2} + \frac{x^4}{4!} + \cdots,$$

the family solution of equation (1) is obtained

$$\begin{pmatrix} q_{11} \\ q_{21} \end{pmatrix} = \begin{pmatrix} q_{10} \\ q_{20} \end{pmatrix} + \frac{4\sqrt{\omega}h_0^*}{|h_0|^2 + |h_1|^2 + |h_2|^2} \begin{pmatrix} h_1 \\ h_2 \end{pmatrix},$$
$$(h_0(x,t), h_1(x,t), h_2(x,t))^{'} = \Delta P_{\diamond} Q_{\diamond} Z, \tag{19}$$

where

$$P = \exp(-\frac{ia_1x}{2})\begin{pmatrix} 1+\omega x & c_1x & c_2x \\ -c_1x & -\frac{xc_1^2\omega-c_1^2+c_2^2\exp(-x\omega)}{\omega^2} & -c_1c_2\frac{x\omega-1+\exp(-x\omega)}{\omega^2} \\ -c_2x & -c_1c_2\frac{x\omega-1+\exp(-x\omega)}{\omega^2} & -\frac{xc_2^2\omega-c_2^2+c_1^2\exp(-x\omega)}{\omega^2} \end{pmatrix}, \tag{20}$$

and

$$Q = \begin{pmatrix} Q_{[11]} & Q_{[12]} & Q_{[13]} \\ -Q_{[12]} & -\frac{c_2^2YE+c_1^2X}{2\omega^2} & -\frac{c_1c_2(YE+X)}{2\omega^2} \\ -Q_{[13]} & -\frac{c_1c_2(YE+X)}{2\omega^2} & -\frac{c_1^2YE+c_2^2X}{2\omega^2} \end{pmatrix}, \tag{21}$$

with

$$\begin{cases} Q_{[11]} = 1 - 12i\omega^4t - 24a_1\omega^3t + (12ia_1^2t - it)\omega^2 + (4a_1^3t - a_1t)\omega, \\ Q_{[12]} = -12itc_1\omega^3 - 24tc_1a_1\omega^2 + (12ia_1^2c_1t - ic_1t)\omega + 4tc_1a_1^3 - tc_1a_1, \\ Q_{[13]} = -12itc_2\omega^3 - 24tc_2a_1\omega^2 + (12ia_1^2c_2t - ic_2t)\omega + 4tc_2a_1^3 - tc_2a_1, \\ E = \exp(2^{-1}t(ia_1^4 - 12ia_1^2\omega^2 + 6i\omega^4 - ia_1^2 + 3i\omega^2 + 2a_1\omega)), \\ X = 24ia_1^2\omega^2t - 24i\omega^4t + 8a_1^3\omega t - 48a_1\omega^3t - 2it\omega^2 - 2a_1\omega t - 2, \\ Y = ia_1^4t - 4i\omega^4t + 8a^3\omega t - 32a\omega^3t - ia_1t + 2it\omega^2 - 2. \end{cases}$$

The non-zero wave number solution we obtained. which is difference in the direction and speed of respiratory wave propagation from the zero wave number solution. When $a_1 = 0$, the solution is same as the next first-order rogue wave solution.

4 Higher-order rogue waves solutions

In this section, the higher-order rogue wave solutions will be studied. For simplicity, taking $\lambda = i\omega(1+\varepsilon), (\varepsilon \to 0)$, then

$$\begin{cases} P(\lambda)|_{\lambda=i\omega(1+\varepsilon)} = \sum_{n=0}^{\infty} P_n\varepsilon^n, \\ Q(\lambda)|_{\lambda=i\omega(1+\varepsilon)} = \exp(-\frac{3it}{2}(2\omega^2+1)\omega^2)\sum_{n=0}^{\infty} Q_n\varepsilon^n, \end{cases} \tag{22}$$

where

$$P_n = \begin{pmatrix} \aleph_n & c_1\omega^{-1}Y_n & c_2\omega^{-1}Y_n \\ -c_1\omega^{-1}Y_n & \omega^{-2}[c_1^2B_n - c_2^2\exp(-\omega x)H_n] & c_1c_2\omega^{-2}[B_n - \exp(-\omega x)H_n] \\ -c_2\omega^{-1}Y_n & c_1c_2\omega^{-2}[B_n - \exp(-\omega x)H_n] & \omega^{-2}[c_2^2B_n - c_1^2\exp(-\omega x)H_n] \end{pmatrix}, \tag{23}$$

with

$$\begin{aligned} &\aleph_n = \mathrm{X}_n + \mathrm{Y}_n + \mathrm{Y}_{n-1}, && B_n = \mathrm{X}_n - \mathrm{Y}_n - \mathrm{Y}_{n-1}, \\ &\mathrm{X}_n = \sum_{m=0}^{[n/2]} C_{n-m}^m 2^{n-2m} H_{2(n-m)}, && \mathrm{Y}_n = \sum_{m=0}^{[n/2]} C_{n-m}^m 2^{n-2m} H_{2(n-m)+1}, \\ &C_n^m = \frac{n!}{m!(n-m)!}, && H_m = \frac{(\omega x)^m}{m!}, \end{aligned} \tag{24}$$

and

$$Q_n = \begin{pmatrix} \hbar_n & -c_1\omega^{-1}\gamma_n & -c_2\omega^{-1}\gamma_n \\ c_1\omega^{-1}\gamma_n & (c_1^2\chi_n + c_2^2\exp(i\omega(10\omega+1)t/2)\rho_n) & c_1c_2(\chi_n - \exp(i\omega(10\omega+1)t/2)\rho_n) \\ c_2\omega^{-1}\gamma_n & c_1c_2(B_n - \exp(i\omega(10\omega+1)t/2)\rho_n) & (c_2^2\chi_n + c_1^2\exp(i\omega(10\omega+1)t/2)\rho_n) \end{pmatrix}, \tag{25}$$

with

$$\begin{aligned} &\hbar_n = \gamma_n - \theta_n - \theta_{n-1}, \qquad \chi_n = \gamma_n + \theta_n + \theta_{n-1}, \\ &\gamma_n = \sum_{\iota=0}^{[3n/4]}\sum_{m=0}^{[\iota]}(-1)^{n-\iota}C_{n-\iota}^{m}C_{2(n-\iota)}^{\iota-m}2^{n-\iota-m}I_{2(n-\iota)}, \\ &\theta_n = i\sum_{\iota=0}^{[(3n+1)/4]}\sum_{m=0}^{[\iota]}(-1)^{n-\iota}C_{n-\iota}^{m}C_{2(n-\iota)+1}^{\iota-m}2^{n-\iota-m}I_{2(n-\iota)+1}, \\ &\rho_n^m = \sum_{n=0}^{[n/2]}C_{n-\iota}^{\iota}i^{n-\iota}2^{n-2\iota}I_n, \qquad I_m = \frac{12i^m\omega^{4m}t^m - \omega^{2m}t^m}{m!}, \end{aligned}$$

According to the above expression, ι is a non-negative integer. Next, to separate the higher order rogue waves, the complex constant vector Z accepts the following expression

$$z_\xi(\varepsilon) = \sum_{\xi=0}^{\infty}Z_\xi\varepsilon^\xi = \sum_{\xi=0}^{\infty}(h_{0\xi}, h_{1\xi}, h_{2\xi})\varepsilon^\xi, \qquad \xi \in N \tag{26}$$

$$\sum_{\xi=0}^{\infty}(h_{0\xi}, h_{1\xi}, h_{2\xi})\varepsilon^\xi = \exp(iP(\lambda)X + iQ(\lambda)T)\beta|_{i(1+\varepsilon)}, \tag{27}$$

and

$$X = \sum_{n=0}^{\infty}R_n\varepsilon^n, \qquad T = \sum_{n=0}^{\infty}S_n\varepsilon^n, \qquad \beta = (\beta_1, \beta_2, \beta_3)^{'}. \tag{28}$$

Accordingly, using the Taylor expansion for the solution (12), we get

$$\begin{aligned} &\Phi|_{\lambda=i\sqrt{\omega}(1+\varepsilon)} = \sum_{n=0}^{\infty}\Phi_n\varepsilon^n, \\ &\Phi_n = \exp(-\frac{3it}{2}(2\omega+1)\omega)\sum_{\xi=0}^{n}\sum_{n_1}^{n}\Delta P_\xi Q_{n_1}(h_{0,n-\xi-n_1}, h_{1,n-\xi-n_1}, h_{2,n-\xi-n_1})^{'}. \end{aligned} \tag{29}$$

When $N = 1$,the first-order rogue wave solutions is obtained

$$\begin{pmatrix} q_1^{[1]} \\ q_2^{[1]} \end{pmatrix} = \begin{pmatrix} q_1^{[0]} \\ q_2^{[0]} \end{pmatrix} + \frac{4\omega h_0^*}{|h_0^{[0]}|^2 + |h_1^{[0]}|^2 + |h_2^{[0]}|^2}\begin{pmatrix} h_1^{[0]} \\ h_2^{[0]} \end{pmatrix} \tag{30}$$

with

$$\Phi_0 = \exp(-\frac{3it}{2}(2\omega^2+1)\omega^2)\begin{pmatrix} h_0^{[0]}(x,t) \\ h_2^{[0]}(x,t) \\ h_2^{[0]}(x,t) \end{pmatrix} = \Delta P_0 Q_0 Z_0,$$

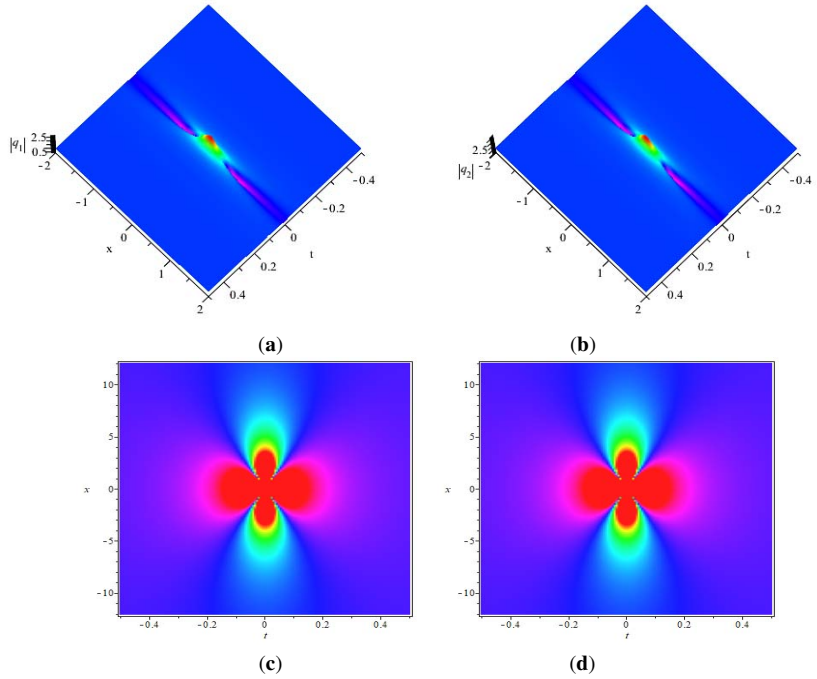

Fig. 3 (Color online) First-order rogue wave in the vector Lakshmanan-Porsezian-Daniel equation(1) for parameters: $a_1 = 0, c_1 = 1 c_2 = 1, h_0 = 1, h_1 = 1, h_2 = 1$. **(a)** and **(c)** are the q_1 are the 3D surface plots of first-order rogue wave, **(b)** and **(d)** are the q_2 are the contour plots of first-order rogue wave.

where

$$P_0 = \begin{pmatrix} 1+\omega x & c_1 x & c_2 x \\ -c_1 x & -\frac{x c_1^2\omega - c_1^2 + c_2^2 \exp(-x\omega)}{\omega^2} & -c_1 c_2 \frac{x\omega - 1 + \exp(-x\omega)}{\omega^2} \\ -c_2 x & -c_1 c_2 \frac{x\omega - 1 + \exp(-x\omega)}{\omega^2} & -\frac{x c_2^2\omega - c_2^2 + c_1^2 \exp(-x\omega)}{\omega^2} \end{pmatrix}, \tag{31}$$

$$Q_0 = \begin{pmatrix} -12i\omega^4 t - i\omega^2 t + 1 & -12i\omega^3 c_1 t - i\omega c_1 t & -12i\omega^3 c_2 t - i\omega c_2 t \\ 12i\omega^3 c_1 t + i\omega c_1 t & Q_0[22] & Q_0[23] \\ 12i\omega^3 c_2 t + i\omega c_2 t & Q_0[23] & Q_0[33] \end{pmatrix}, \tag{32}$$

where

$$\begin{cases} Q_0[22] = \left(12i\omega^4 c_1^2 t + i c_1^2 \omega^2 t + c_1^2 + c_2^2 \exp\left(\frac{it\omega^2(10\omega^2+1)}{2}\right)\right)\omega^{-2}, \\ Q_0[23] = \left(-c_1 c_2 (12\omega^4 t + \exp\left(\frac{it\omega^2(10\omega^2+1)}{2}\right) + \omega^2 t - 1)\right)\omega^{-2}, \\ Q_0[33] = \left(12i\omega^4 c_2^2 t + i c_2^2 \omega^2 t + c_2^2 + c_1^2 \exp\left(\frac{it\omega^2(10\omega^2+1)}{2}\right)\right)\omega^{-2}. \end{cases} \tag{33}$$

Fig.3 shows the rogue wave for equation(1) with suitable parameters. The amplitude q_i is peaked when $x = 0$ and $t = 0$, and the contour of the wave is symmetrical

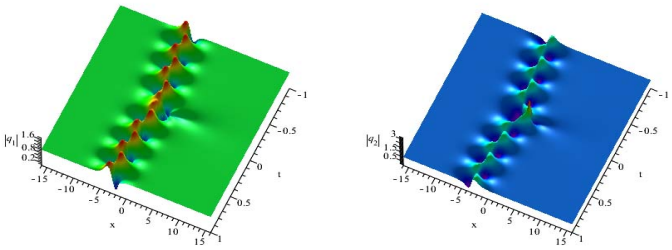

(**a**) (**b**)

Fig. 4 (Color online) One-order rogue waves on breathing bright-dark solitons by choosing suitable parameters: $c_1 = 1c_2 = 1, h_0 = 1, h_1 = 1, h_2 = 1000$.. **(a)** and **(c)** are the q_1 are the 3D surface plots of first-order rogue wave, **(b)** and **(d)** are the q_2 are the contour plots of first-order rogue wave.

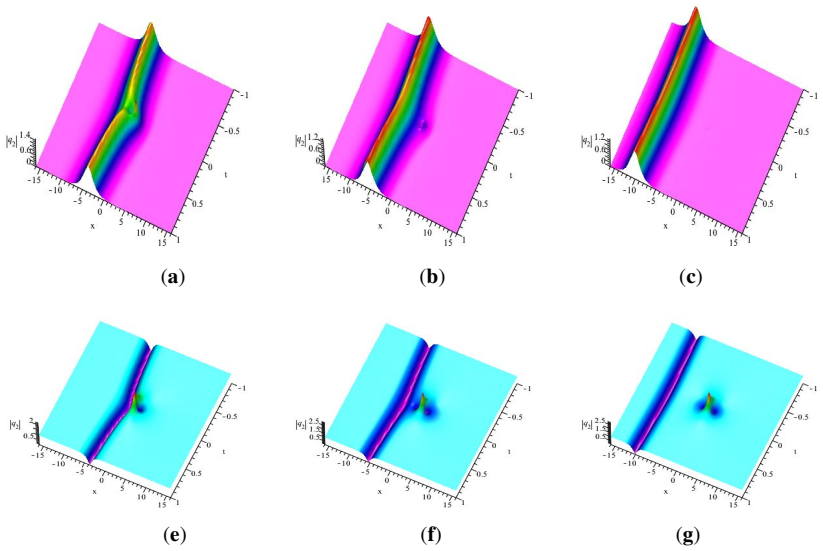

(**a**) (**b**) (**c**)

(**e**) (**f**) (**g**)

Fig. 5 (Color online) One-order rogue waves on breathing bright-dark solitons by choosing suitable parameters: $c_1 = 0, c_2 = 1, h_0 = 1, h_1 = 1$. **(a)** $h_2 = 1$, **(b)** $h_2 = 100$, **(b)** $h_2 = 1000$,.

about the t-axis. Fig.4 shows that the Peregrine bump coexists and interacts with-breather-like solitons. Form the figures, we note that the soliton slightly bends towards the rogue wave. Such solutions are generated by using the seeding solutions as the plane waves ($c_1 \neq 0$ and $c_2 \neq 0$). A complicated breather-like pulse is produced by the superposition of the dark and bright contributions. It is found that the peak height in the q_1 component is lower than the peak height in the q_2 component in Fig 5. According to Fig.4 and Fig.5, when$c_1 c_1 \neq 0$, the interference between dark and bright components leads to Fig.5 shows a vector dark-bright soliton together with a single Peregrine soliton. As shown in the Fig.5 (a) and (b) and (c),we note that increasing the h_2, the boomeron-type bright solitons is disappear and the Peregrine structure is

about to die away, and according the Fig.5 (*d*) and (*e*) and (*f*) decreasing the h_2 the rogue wave stay away from the dark solitons and generating the boomeron-type dark solitons.

when $N = 2$,the second-order rogue wave solutions is obtained

$$\begin{pmatrix} q_1^{[2]} \\ q_2^{[2]} \end{pmatrix} = \begin{pmatrix} q_1^{[1]} \\ q_2^{[1]} \end{pmatrix} + \frac{4\omega h_0^*}{|h_0^{[1]}|^2 + |h_1^{[1]}|^2 + |h_2^{[1]}|^2} \begin{pmatrix} h_1^{[1]} \\ h_2^{[1]} \end{pmatrix} \tag{34}$$

with

$$\begin{aligned}
&\Phi_1 = \exp(-\frac{3it}{2}(2\omega^2+1)\omega^2)(\Delta P_1 Q_0 Z_0 + \Delta P_0 Q_1 Z_0 + \Delta P_0 Q_0 Z_1), \\
&\begin{pmatrix} h_0^{[1]}(x,t) \\ h_2^{[1]}(x,t) \\ h_2^{[1]}(x,t) \end{pmatrix} = R^{[1]}\Phi_2 + i\sqrt{\omega}\Phi_1, \\
&R^{[1]} = 2i\sqrt{\omega}(I_3 - T^{[1]}), \qquad T^{[1]} = \frac{\Phi_0 \Phi_0^*}{\Phi_0 * \Phi_0}.
\end{aligned}$$

where

$$\begin{aligned}
&\Phi_2 = \begin{pmatrix} h_{02}(x,t) \\ h_{12}(x,t) \\ h_{22}(x,t) \end{pmatrix} = \Delta P_2 Q_2 Z_2, \qquad Z_2 = \begin{pmatrix} \alpha_{12} \\ \alpha_{22} \\ \alpha_{32} \end{pmatrix}, \\
&P_1 = \begin{pmatrix} \frac{\omega^3 x^3}{3} + \omega^2 x^2 + \omega x & \frac{c_1\omega^2 x^3}{3} & \frac{c_2\omega^2 x^3}{3} \\ -\frac{c_1\omega^2 x^3}{3} & P_1[22] & P_1[23] \\ -\frac{c_2\omega^2 x^3}{3} & P_1[23] & P_1[33] \end{pmatrix},
\end{aligned} \tag{35}$$

$$Q_1 = \begin{pmatrix} Q_1[11] & c_1 Q_1[13] & Q_1[13] \\ -c_1 Q_1[13] & Q_1[22] & Q_1[23] \\ -Q_1[13] & Q_1[23] & Q_1[33] \end{pmatrix},$$

with

$$\begin{cases}
P_1[22] = -\dfrac{x\left(c_1^2\omega^2 x^2 - 3c_1^2\omega x + 3c_1^2 + 3c_2^2\exp(-x\omega)\right)}{3\omega}, \\
P_1[23] = -\dfrac{xc_1c_2\left(\omega^2 x^2 - 3\omega x + 3 - 3\exp(-x\omega)\right)}{3\omega}, \\
P_1[33] = -\dfrac{x\left(c_2^2\omega^2 x^2 - 3c_2^2\omega x + 3c_2^2 + 3c_1^2\exp(-x\omega)\right)}{3\omega},
\end{cases} \tag{36}$$

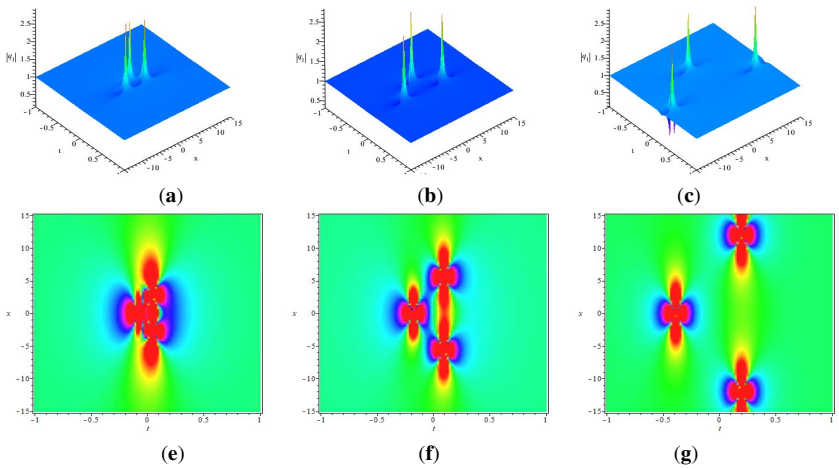

Fig. 6 (Color online) Second-order rogue waves on breathing bright-dark solitons by choosing suitable parameters: $c_1 = 1, c_2 = 1, t_0 = 1$. **(a)** $t_1 = 1$, **(b)** $t_1 = 10$, **(c)** $t_1 = 1000$,.

$$
\begin{cases}
Q_1[11] = \left(576i\omega^{12} + 144i\omega^{10} + 12i\omega^8 + \dfrac{i\omega^6}{3}\right)t^3 - \left(144\omega^8 + 48\omega^6 + 3\omega^4\right)t^2 - \left(40i\omega^4 + 4i\omega^2\right)t, \\
Q_1[12] = c_1\left(576i\omega^{11} + 144i\omega^9 + 12i\omega^7 + \dfrac{i\omega^5}{3}\right)t^3 - c_1\left(24\omega^5 + 2\omega^3\right)t^2 - c_1\left(28i\omega^3 + i\omega\right)t, \\
Q_1[13] = c_2\left(576i\omega^{11} + 144i\omega^9 + 12i\omega^7 + \dfrac{i\omega^5}{3}\right)t^3 - c_2\left(24\omega^5 + 2\omega^3\right)t^2 - c_2\left(28i\omega^3 + i\omega\right)t, \\
Q_1[22] = c_1^2\left(-576i\omega^{10} - 144i\omega^8 - 12i\omega^6 - \dfrac{\omega^4}{3}i\right)t^3 - c_1^2\left(144\omega^6 - \omega^2\right)t^2 \\
\qquad + c_1^2 40i\omega^2 t + 32ic_2^2\omega^2 \exp(\dfrac{it\omega^2(10\omega^2+1)}{2})t, \\
Q_1[23] = c_1c_2\left(576\omega^{10} + 144\omega^8 + 12\omega^6 + \dfrac{\omega^4}{3}\right)t^3 - c_1c_2\left(144\omega^6 - 24i\omega^4 + 24\omega^4 - 2i\omega^2 + \omega^2\right)t^2 \\
\qquad - c_1c_2\left(40\omega^2 + 2i + 2\right)t - 32ic_1c_2\omega^2 \exp(\dfrac{it\omega^2(10\omega^2+1)}{2})t, \\
Q_1[33] = c_2^2\left(-576i\omega^{10} - 144i\omega^8 - 12i\omega^6 - \dfrac{\omega^4}{3}i\right)t^3 - c_2^2\left(144\omega^6 - \omega^2\right)t^2 \\
\qquad + c_2^2 40i\omega^2 t + 32ic_1^2\omega^2 \exp(\dfrac{it\omega^2(10\omega^2+1)}{2})t.
\end{cases}
\tag{37}
$$

According to the calculation, when $c_1 = c_2 = 1$, the second-order rogue wave q_1 equal q_2, and the distance between the three peaks become increases as t_1 increases (see Figs.6). Here, we only plot q_1. Fig. 7 (a) to (c) reveals the interaction between

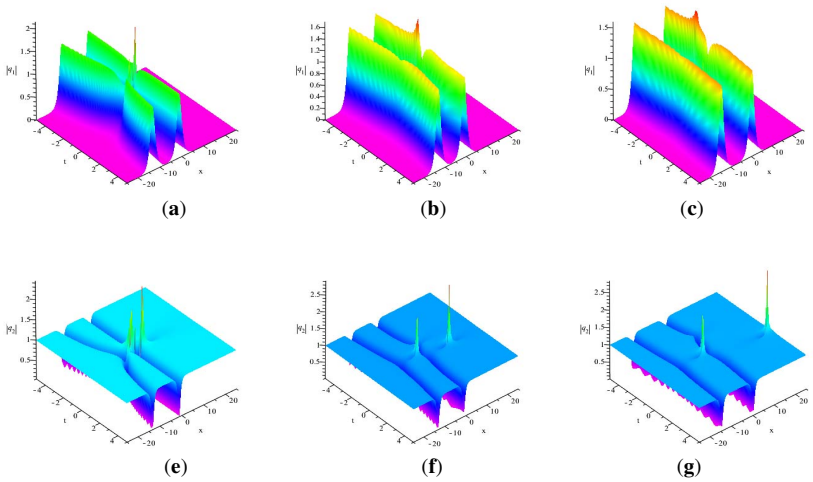

Fig. 7 (Color online) Second-order rogue waves on breathing bright-dark solitons by choosing suitable parameters: $c_1 = 0, c_2 = 1, t_0 = 0$. **(a)** $t_1 = 1$, **(b)** $t_1 = 100$, **(b)** $t_1 = 1000$,.

second-order rogue waves and bright-soliton waves. Fig. 7 (d) to (f) displays the interaction between second-order rogue waves and dark-soliton waves.

5 Conclusions

In conclusion, the rational solutions of the vector Lakshmanan-Porsezian-Daniel equation(1) has been investigated via the DDT with Lax pair. In order to help the reader to better understand the rational solution, the new breather wave and new rogue wave solutions are drawn by looking for the appropriate parameters (Figure 1 to Figure 7). All figures in this paper are drawn according to the explicit analytical formulas of solutions. When $\lambda \neq i\omega$ and selecting appropriate parameters, Figure 1 and 2 show the AB wave and KMs under bright-dark soliton background. When $\lambda = i\omega$, Figures 4 to 7 show the interaction between rogue waves and dark-bright soliton waves. These presented phenomena should be used to predict rogue wave phenomena in optics, fluid, dynamics, BECs, and finance, etc

Acknowledgments

This work was supported by the National Natural Science Foundation of China (No. 71690242, No. 11731014).

Conflict of interest No potential conflict of interest was reported by the authors

References

1. Christian Kharif, Efim Pelinovsky, Alexey Slunyaev. Rogue Waves in the Ocean[M]. Springer Berlin Heidelberg, 2009.
2. Alfred Osborne. Nonlinear Ocean Waves & the Inverse Scattering Transform. academic pr inc, 2010.
3. Onorato M , Residori S , Bortolozzo U ,Montina A and Arecchi F T. Rogue waves and their generating mechanisms in different physical contexts. Phys. Rep, 2013, 528(2):47-89.
4. Chabchoub A , Hoffmann N P , Akhmediev N . Rogue Wave Observation in a Water Wave Tank. Phys. Rev. Lett, 2011, 106(20):142-145.
5. Moslem W M , Shukla P K , Eliasson B . Surface plasma rogue waves. EPL (Europhysics Letters). 2011, 96(2):25002.
6. Bludov Y V , Konotop V V , Akhmediev N . Matter rogue waves. Phys. Rev. A. 2009, 80(3), 033610.
7. Zhen-Ya Y. Financial rogue waves. Commun.Theor.Phys.2010, 54(5): 947.
8. Zhen-Ya Y.Financial Rogue Waves Appearing in the Coupled Nonlinear Volatility and Option Pricing Model[J]. Phys.Lett.A. 2011,375:4274-4279.
9. Ablowitz M J, Clarkson PA. Solitons, nonlinear evolution equations and inverse scattering. Cambridge Univ. Pr, 1991.
10. Ablowitz M J , Kaup D J , Newell A C , Segur A C. Nonlinear-Evolution Equations of Physical Significance. hys. Rev. Lett. 1973, 31(2):125-127.
11. Matveev, V B, Salle M A. Darboux transformations and solitons. springer, 1991.
12. Hirota R. Exact Solution of the Korteweg-de Vries Equation for Multiple Collisions of Solitons. Phys. Rev. Lett. 1971, 27(18):1192-1194.
13. Wang D S , Wei X . Integrability and exact solutions of a two-component KortewegCde Vries system[J]. Applied Mathematics Letters, 2015:S0893965915002219.
    D. S. Wang, X. Wei, *Integrability and exact solutions of a two-component Korteweg-de Vries system*, Appl. Math. Lett, **51**, 60-67 (2016).
14. Tao X , Yong C . Semirational solutions to the coupled Fokas-Lenells equations[J]. Nonlinear Dynamics, 2018. T. Xu, Y. Chen, *Semirational solutions to the coupled Fokas-Lenells equations*. 2019.
15. Liu W H, Zhang Y F, Shi D D. Dynamics of breather waves and rogue waves on a soliton background in the coupled Hirota systems. Math. Mtthod. Appl. Sci. 2019.
16. Dudley J M , Dias, Frdric, Erkintalo M, Genty G. Instabilities, breathers and rogue waves in optics. Nature Photonics, 2014, 8(10):755-764.
17. Benjamin T B , Feir J E . The disintegration of wave trains on deep water. J. Fluid. Mech. 1967, 27:417-430.
18. Yanchow, Ma. The Perturbed Plane-Wave Solutions of the Cubic Schrödinger Equation. Stud. App. Math.1979,60:43-58.
19. Ye Y L, Hou C, Cheng D D, Chen S H. Rogue wave solutions of the vector Lakshmanan-Porsezian-Daniel equation, Phy. Lett. A.2020, 384(11).
20. Xu T , He G . Higher-order interactional solutions and rogue wave pairs for the coupled Lakshmanan-Porsezian-Daniel equations. Nonlinear, Dynam. 2019, 98(3):1731-1744.
21. Chen S , Mihalache D . Vector rogue waves in the Manakov system: diversity and compossibility.J. Phy. A Math. 2015, 48(21):215202.
22. Wang X B, H B . Characteristics of rogue waves on a soliton background in a coupled nonlinear Schrödinger equation. Math. Mtthod. Appl. Sci.2019, 42(8): 2586-2596.
23. Baronio F, Degasperis A,Conforti M, Wabnitz S, Solutions of the Vector Nonlinear Schrödinger Equations: Evidence for Deterministic Rogue Waves, Phys. Rev. Lett. 2012, 109(4): 044102.
24. Guo B L, Lin L M. Rogue Wave, Rogue Wave, Breathers and Bright-Dark-Rogue Solutions for the Coupled Schrödinger Equations. Chinese. Phy. Lett, 2011, 28(11).
25. Du Z, Tian B, Chai H P, Zhao X H. Lax pair, Darboux transformation, vector rational and semi-rational rogue waves for the three-component coupled Hirota equations in an optical fiber. Eur. Phys. J. Plus, 2019, 134(5).
26. Ye Y , Zhou Y , Chen S. General rogue wave solutions of the coupled FokasCLenells equations and non-recursive Darboux transformation. Proc. Math. Phy, 2019, 475(2224).
27. Xu T , He G . Higher-order interactional solutions and rogue wave pairs for the coupled Lakshmanan-Porsezian-Daniel equations. Nonlinear. Dynam. 2019, 98(3):1731-1744.